Available online at www.sciencedirect.com
ScienceDirect
Polyhedron 26 (2007) 1845–1848
POLYHEDRON
www.elsevier.com/locate/poly

New derivatives of an enneanuclear Mn SMM

Muralee Murugesu [a], Wolfgang Wernsdorfer [b], George Christou [a], Euan K. Brechin [c,*]

[a] *Department of Chemistry, University of Florida, Gainesville, FL 32611-7200, USA*
[b] *Laboratoire Louis Néel-CNRS, 38042 Grenoble, Cedex 9, France*
[c] *School of Chemistry, The University of Edinburgh, EH9 3JJ, UK*

Received 4 September 2006; accepted 19 September 2006
Available online 29 September 2006

Abstract

The reaction of the neutral triangular species $[Mn_3O(O_2CR)_6L_3]$ (R = Me, Ph, CMe_3; L = py) with the tripodal ligands H_3tmp (1, 1, 1-tris(hydroxymethyl)propane) and H_4peol (pentaerythritol) affords the enneanuclear complexes $[Mn_9O_7(O_2CMe)_{11}(tmp)(py)_3(H_2O)_2]$ (**2**); $[Mn_9O_7(O_2CMe)_{11}(Hpeol)(py)_3(H_2O)_2]$ (**3**); $[Mn_9O_7(O_2CCMe_3)_{11}(Hpeol)(py)_3(H_2O)_2]$ (**4**); and $[Mn_9O_7(O_2CPh)_{11}(Hpeol)(py)_3(H_2O)_2]$ (**5**). Complexes **2**–**5** are characterized by spin ground states of $S = 17/2$ with axial zero-field splitting parameters in the range $D = -0.26$–$0.30\ cm^{-1}$. Sweep-rate and temperature dependent hysteresis loops diagnostic of SMM behaviour are observed below 1.2 K featuring steps at regular intervals of field.

Keywords: Maganese; SMMs; Clusters; High spin ground states; Tripodal alcohols

Polymetallic clusters containing multiple Mn(III) ions have proven to be the most fruitful source of single-molecule magnets (SMMs) [1–3]. There are two main reasons for this: (a) Jahn–Teller distorted Mn(III) ions provide the source of single ion anisotropy and, (b) the ability of Mn to exist in a variety of oxidation states means that the (primarily) mixed-valent polynuclear clusters produced will, more often than not, display non-zero spin ground states even if the dominant exchange interactions are antiferromagnetic in nature [4]. However, there exists few 'simple', readily available, soluble sources of Mn(III) and thus synthetic strategies toward making polymetallic complexes containing Mn(III) ions have involved either, the oxidation of Mn(II) species, the reduction of Mn(IV) or Mn(VII) species, and the use of small (or in some cases, large) preformed Mn(II)/Mn(III)/Mn(IV) containing clusters such as $[Mn_3O(O_2CR)_6L_3]^{0/+}$ or $[Mn_{12}O_{12}(OAc)_{16}(H_2O)_4]$, in the presence of flexible organic bridging ligands such as carboxylates and alkoxides, *via* self-assembly. This has been achieved both chemically and electrochemically [1].

We have been exploring the reactivity of tripodal alcohol ligands in the synthesis of 3d transition metal SMMs [5]. When fully deprotonated the disposition of the three alkoxide arms of the tri-anion generally directs the formation of triangular $[M_3]$ units, where each arm of the ligand bridges one edge of the triangle. In the presence of co-ligands such as carboxylates or β-diketonates, these smaller units can combine in diverse ways to produce complexes whose structures range from 'simple' $[M_3]$ or $[M_4]$ (centered) triangles to rod-like complexes describing 'one-dimensional' arrays of edge-sharing triangles; planar disc-like complexes describing 'two-dimensional' arrays of edge-sharing triangles; and more complicated 'three-dimensional' arrays commonly based on tetrahedra, octahedra and icosahedra [5,6]. One such complex $[Mn_9O_7(O_2CMe)_{11}(thme)(py)_3(H_2O)_2]$ (**1**) [7] (H_3thme = 1,1,1-tris(hydroxymethyl)ethane), whose structure describes part of an idealised icosahedron, was made from the simple reaction between the triangle $[Mn_3O(O_2CMe)_6py_3]$ and H_3thme in MeCN. This is an intriguing

* Corresponding author.
E-mail address: ebrechin@staffmail.ed.ac.uk (E.K. Brechin).

0277-5387/$ - see front matter © 2006 Elsevier Ltd. All rights reserved.
doi:10.1016/j.poly.2006.09.063

SMM not simply because of its ease of synthesis and stability in solution but because it displays beautiful hysteresis loops in single crystal *M versus H* studies that possess well defined steps at regular intervals of field indicative of magnetic quantum tunneling [8].

We therefore decided to attempt to make further derivatives of complex **1**, and herein report the syntheses, structures and initial magnetic properties of four such molecules. The complexes $[Mn_9O_7(O_2CMe)_{11}(tmp)(py)_3(H_2O)_2]$ (**2**); $[Mn_9O_7(O_2CMe)_{11}(Hpeol)(py)_3(H_2O)_2]$ (**3**); $[Mn_9O_7(O_2CPh)_{11}(Hpeol)(py)_3(H_2O)_2]$ (**4**); and $[Mn_9O_7(O_2CCMe_3)_{11}(Hpeol)(py)_3(H_2O)_2]$ (**5**) (H_3tmp = 1,1,1-tris(hydroxymethyl)propane; H_4peol = pentaerythritol) are all made in an identical manner, *via* the reaction of the appropriate $[Mn_3O(O_2CR)_6L_3]^{0/+}$ triangle with the appropriate tripodal alcohol in MeCN. All five crystallize in the monoclinic space group $P2(1)/n$.

The metallic skeletons of **2**–**5** (Fig. 1) comprise a series of ten-edge-sharing triangles that describes part of an idealized icosahedron in which three of the twelve vertices are missing. The $[Mn^{IV}_3Mn^{III}_4Mn^{II}_2O_7]^{14+}$ central core can be described as either a series of vertex- and edge-sharing $[Mn_3O]$ units, or perhaps most easily as a $[Mn^{III}_4Mn^{II}_2O_6]^{4+}$ ring on which is sitting a smaller $[Mn^{IV}_3O]^{10+}$ ring. The upper $[Mn_3O]^{10+}$ ring consists only of Mn(IV) ions and is capped on one side by the sole tripodal ligand each O-arm of which acts as a μ-bridge, and on the other side by a μ_3-oxide. The $[Mn^{IV}_3O]^{10+}$ unit is connected to the $[Mn^{III}_4Mn^{II}_2O]^{4+}$ ring *via* six μ_3-oxides within the six-membered wheel and three carboxylates which bridge in their familiar *syn*, *syn*, μ-mode. The remaining carboxylates in the structure bridge between the Mn ions in the $[Mn^{III}_4Mn^{II}_2O_6]^{4+}$ ring in the same manner. The remaining coordination sites are occupied by two water molecules and three pyridines. All the Mn ions are in distorted octahedral geometries, with their oxidation states assigned using charge balance considerations, bond lengths and bond valence sum (BVS) calculations. The Jahn–Teller elongations of the Mn(III) ions all lie approximately perpendicular to the plane of the $[Mn^{III}_4Mn^{II}_2O_6]^{4+}$ ring.

Variable temperature magnetic susceptibility data were collected on **2**–**5** in the temperature range 300–1.8 K in an applied field of 1 kG. For each complex the observed behavior is similar [9]. The room temperature value of $\chi_M T$ of approximately 18 cm^3 K mol^{-1} remains constant until around 200 K where it begins to increase to a maximum value of approximately 37 cm^3 K mol^{-1}at 20 K, before dropping sharply below this temperature. The spin only (g = 2) value for a $[Mn^{IV}_3Mn^{III}_4Mn^{II}_2]$ unit is approximately 30 cm^3K mol^{-1}.The maximum in $\chi_M T$ is indicative of a $S = 17/2 \pm 1$ spin ground state, with the low temperature decrease assigned to zero-field splitting, Zeeman effects and/or intermolecular antiferromagnetic interactions. Magnetization data collected in the ranges 10–70 kG and 1.8–4.0 K for **5** are plotted as reduced magnetization ($M/N\mu_B$) *versus* H/T in Fig. 2. For a complex entirely populating the ground state and experiencing no zero-field splitting, the observed isofield lines should

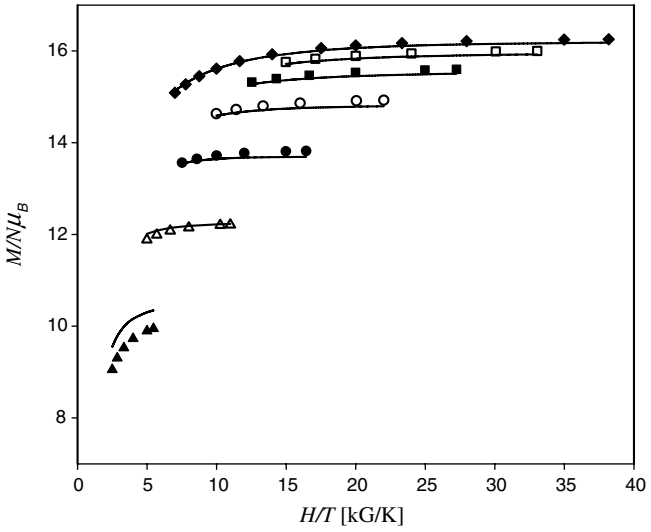

Fig. 2. Plot of reduced magnetization *vs.* H/T for **5**. The solid lines are the fit of the data. See text for details.

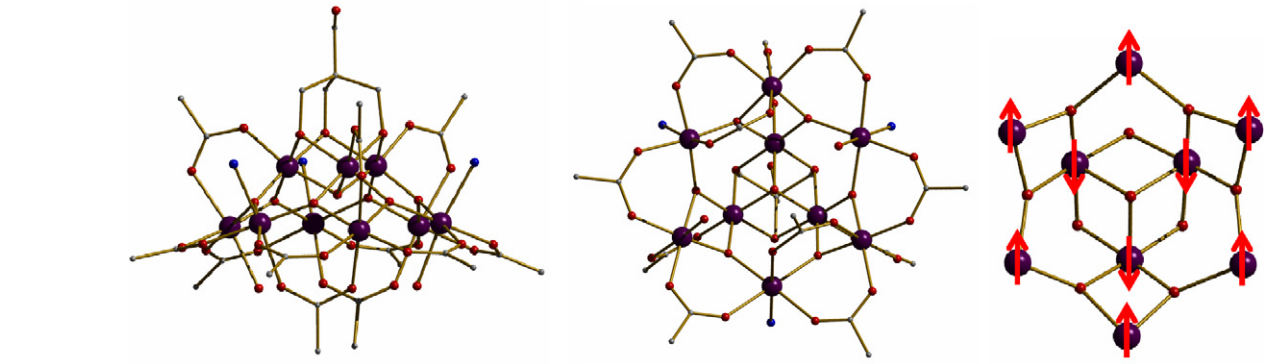

Fig. 1. The molecular structure of complex **5**, viewed parallel (left) and perpendicular (middle) to the $[Mn^{III}_4Mn^{II}_2O_6]^{4+}$ ring; the Me groups of the O_2CCMe_3 ligands and the C atoms of the pyridines have been removed for clarity. The metal–oxygen core common to complexes **1**–**5**, showing the proposed spin topology (right). Colour code: Mn, purple; O, red; N, blue; C, grey. (For interpretation of the references to color in this figure legend, the reader is referred to the web version of this article.)

superimpose and saturate at a value ($M/N\mu_B$) equal to gS. This is clearly not the case and is suggestive of appreciable ZFS. The data were fitted by a matrix-diagonalization method to a model that assumes only the ground state is populated, includes axial zero-field splitting ($D\hat{S}_z^2$), and carries out a full powder average [10]. The best fit gave $S = 17/2$, $g = 1.98$ and $D = -0.27\ cm^{-1}$. The ground state can be rationalized by assuming an antiferromagnetic interaction between the ferromagnetically coupled Mn(IV) ions in the $[Mn_3^{IV}O]^{10+}$ ring and the Mn(III/II) ions in the $[Mn_4^{III}Mn_2^{II}O_6]^{4+}$ ring (Fig. 1).

The in-phase ($\chi'_M T$) and out-of-phase (χ''_M) ac susceptibility signals for **5** are shown in Fig. 3. The in-phase signal shows a plateau above *ca.* 5 K indicative of an isolated spin ground state. Extrapolation of this slope to 0 K gives a value of $\sim 37\ cm^3\ K\ mol^{-1}$ suggesting a spin ground state of $S = 17/2 \pm 1$ in agreement with the dc data. There is a frequency-dependent decrease in the $\chi'_M T$ signal and a frequency-dependent out-of-phase signal at $T < 5$ K. The peak at 1000 Hz occurs at approximately 3.5 K. Both are strong indicators of SMM behavior. The S and D values obtained suggest an upper limit to the potential energy barrier (U) to magnetization reversal ($U = (S^2 - 1/4)|D|$) of ~28 K. This was confirmed by single crystal hysteresis loop and relaxation measurements performed using a micro-SQUID setup [11]. Studies of the magnetization performed at very low temperature and high fields show that all complexes behave as SMMs with long relaxation times. Fig. 4 presents typical magnetization (M) *versus* applied DC field measurements for **5**. Hysteresis loops are observed, whose coercivity is strongly temperature and sweep-rate dependent, increasing with decreasing temperature and increasing field sweep rate, as expected for the superparamagnetic-like behavior of a SMM. The hysteresis

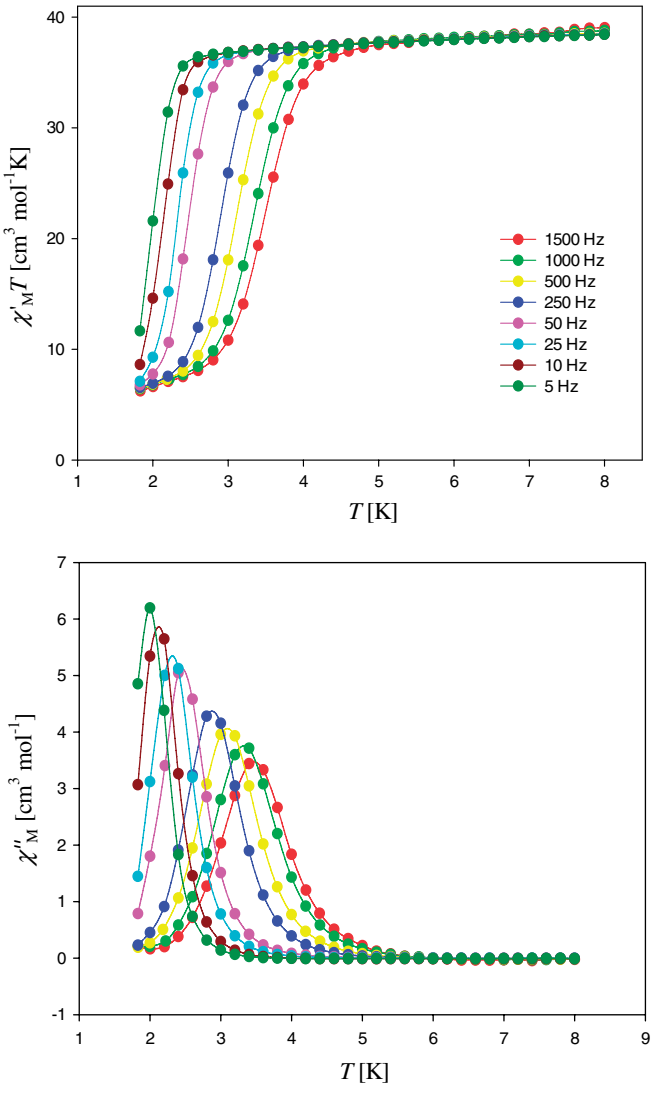

Fig. 3. Plots of the in-phase (χ'_M)) signal as ($\chi'_M T$) and out-of-phase (χ''_M) signal in ac susceptibility studies *vs.* temperature for **5** in a 3.5 G field oscillating at the indicated frequencies.

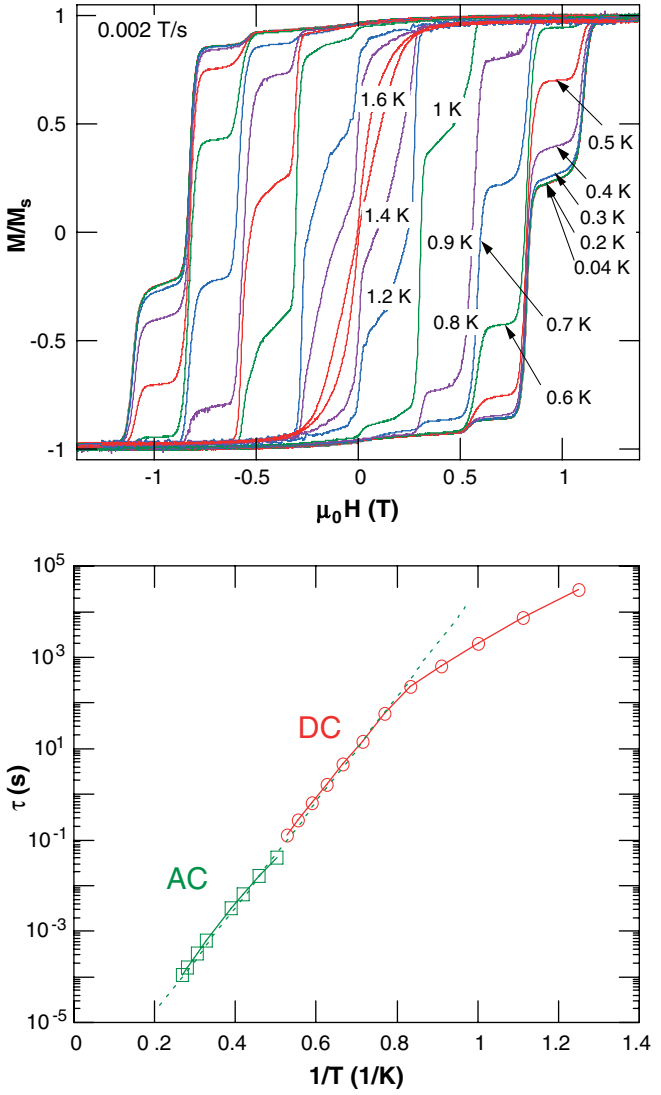

Fig. 4. Single crystal magnetisation (M) *vs.* field (H) hysteresis loops for complex **5** (top) at the indicated field sweep rates and temperatures; the magnetisation is normalised to its saturation value (M_S). Arrhenius plot for **5**; the dashed line is the fit of the thermally-activated region to the Arrhenius equation.

loops show the step-like features indicative of quantum tunneling of magnetization. Relaxation data determined from a combination of single crystal dc relaxation decay measurements and ac measurements on a powdered sample allow the construction of a τ *versus* $1/T$ plot based on the Arrhenius relationship $\tau = \tau_0 \exp(U_{\text{eff}}/kT)$ (Fig. 4). The slope of the thermally-activated region yields an effective energy barrier for the reorientation of the magnetization of 26.5 K with $\tau_0 = 9.6 \times 10^{-8}$ s.

In conclusion, we have successfully made four new analogues of the Mn_9 SMM. These are made *via* analogous reactions choosing the appropriate Mn triangle and the appropriate tripodal ligand in MeCN. Their structures and magnetic properties are similar to the original complex **1** [8]. All display $S = 17/2$ spin ground states and are new examples of high-spin half-integer Mn SMMs. The Mn_9 family have much in common with the prototype Mn SMM $[Mn_{12}O_{12}(O_2CR)_{16}\ (H_2O)_4]^{n-}$ $(n = 1,2)$ family and can be considered their 'baby brothers': not only do they look similar, but in each case the central ferromagnetically coupled Mn(IV) ions couple antiferromagnetically with the surrounding wheel of Mn(III/II) ions, and both have an interchangeable organic 'coat'.

Supplementary material

CCDC 189138 contains the supplementary crystallographic data for **1**–**5**. These data can be obtained free of charge via http://www.ccdc.cam.ac.uk/conts/retrieving.html, or from the Cambridge Crystallographic Data Centre, 12 Union Road, Cambridge CB2 1EZ, UK; fax: (+44) 1223-336-033; or e-mail: deposit@ccdc.cam.ac.uk.

References

[1] G. Aromí, E.K. Brechin, Struct. Bond. 122 (2006) 1.
[2] G. Christou, D. Gatteschi, D.N. Hendrickson, R. Sessoli, MRS Bull. 25 (2000) 66.
[3] G. Christou, Polyhedron 24 (2005) 2065.
[4] (a) See for example: M. Murugesu, M. Habrych, W. Wernsdorfer, K.A. Abboud, G. Christou, J. Am. Chem. Soc. 126 (2004) 4766;
(b) R. Sessoli, H.-L. Tsai, A.R. Schake, S. Wang, J.B. Vincent, K. Folting, D. Gatteschi, G. Christou, D.N. Hendrickson, J. Am. Chem. Soc. 115 (1993) 1804;
(c) D.N. Hendrickson, G. Christou, H. Ishimoto, J. Yoo, E.K. Brechin, A. Yamaguchi, E.M. Rumberger, S.M.J. Aubin, Z. Sun, G. Aromí, Mol. Cryst. Liq. Cryst. 376 (2002) 301;
(d) D.N. Hendrickson, G. Christou, H. Ishimoto, J. Yoo, E.K. Brechin, A. Yamaguchi, E.M. Rumberger, S.M.J. Aubin, Z. Sun, G. Aromí, Polyhedron 20 (2001) 1479.
[5] E.K. Brechin, Chem. Commun. (2005) 5141.
[6] R.T.W. Scott, S. Parsons, M. Murugesu, W. Wernsdorfer, G. Christou, E.K. Brechin, Angew. Chem., Int. Ed. 44 (2005) 6540.
[7] E.K. Brechin, M. Soler, J. Davidson, D.N. Hendrickson, S. Parsons, G. Christou, Chem. Commun. (2002) 2252.
[8] S. Piligkos, G. Rajaraman, M. Soler, N. Kirchner, J. van Slageren, R. Bircher, S. Parsons, H.-U. Güdel, J. Kortus, W. Wernsdorfer, G. Christou, E.K. Brechin, J. Am. Chem. Soc. 127 (2005) 5572.
[9] M. Murugesu, W. Wernsdorfer, G. Christou, E.K. Brechin, in preparation.
[10] E.R. Davidson, MAGNET, Indiana University.
[11] W. Wernsdorfer, Adv. Chem. Phys. 118 (2001) 99.